Jestr

Journal of Engineering Science and Technology Review 17 (2) (2024) 145 - 156

Research Article

JOURNAL OF
Engineering Science and Technology Review

www.jestr.org

Event-triggered Proportional-Integral Control for Flexible Linkage Servo System Using Genetic Algorithm

Zechong Lu[1], Chuansheng Tang[1,2,*], Hui Wang[1] and Tao Li[3]

[1]*College of Mechanical and Electrical Engineering, Zhengzhou University of Light Industry, Zhengzhou 450000, China*
[2]*School of Information and Intelligent Manufacturing, Chongqing City Vocational College, Chognqing 402106, China*
[3]*Department of Informatics, University of Zurich, Zurich, 8050, Switzerland*

Received 10 January 2024; Accepted 28 March 2024

Abstract

A traditional servo system regards the coupling of the motor and load as a rigid connection, it ignores the influence of system flexibility, and thus it hardly meets the requirements of high-precision industrial production. In order to improve the resonance problem caused by flexible coupling in flexible linkage servo systems, this study proposed an event-triggered proportional-integral control for flexible linkage servo system using genetic algorithm. First, a dynamic model of flexible linkage servo system was established, and the system parameters were identified using a multi-innovation stochastic gradient (MISG) algorithm. Second, a genetic algorithm optimized proportional-integral controller with an event-triggered (ET-GA-PI) mechanism was designed, and the genetic algorithm was introduced to optimize the control parameters. Moreover, an event-triggered mechanism with a fixed threshold was adopted to control the update times of the controller. Finally, the simulation experiment was compared with traditional control methods, such as pole placement proportional-integral control, second-order system engineering design proportional-integral control, and multiple-capacity process proportional-integral control. Furthermore, the effectiveness of the control method was verified. Results demonstrate that, the MISG identification algorithm combined with the current and historical speed input and output information of the flexible linkage servo system effectively improves the accuracy of parameter identification (5.8 times higher than the traditional stochastic gradient identification, and the quantization error is reduced by 21.6 times) and the speed of convergence (21.6 times higher than the traditional stochastic gradient identification). The update times of the proposed ET-GA-PI controller are 1/20 of those of the traditional genetic algorithm proportional-integral control, and the overshoot is only 0.1731%. Compared with traditional control, the proposed ET-GA-PI controller needs less communication resources to meet the needs of complex network control systems. The proposed method has practical implications on meeting the requirements of flexible servo systems in high-precision robots and computerized numerical control machine tools and other engineering applications.

Keywords: Event-triggered control, Flexible linkage servo system; Genetic algorithm PI, Multi-innovation parameter identification

1. Introduction

As a control system of industrial production equipment, a servo control system can be widely used in robots, laser processing, automation equipment, and various military weapons with certain positioning accuracy, position tracking, and fast tracking speed. With the rapid development of modern industrial technology, the proposed requirements for servo systems have been increasing, and the study and development of high-performance servo systems have become the focus of colleagues at home and abroad. Conventional direct drive servo systems often treat the motor coupling and output shaft as rigid connections, ignoring the influence of rigid deformation on the system during transmission and thus only meeting the requirements of low precision. Zhou et al. [1] proposed a rigid compensation method for weakly rigid servo control systems with certain adaptive capabilities, which to a certain extent reduced the pseudo vibration caused by the insufficient rigidity of weakly rigid machine tools.

To meet the requirements of high performance and high precision in specific occasions, researchers have investigated flexible servo systems, which have advantages of high performance, high precision, and versatility [2-3]. These systems are applied in industrial heavy-duty flexible robots, solar panels on spacecraft, flexible continuum manipulators, flexible antennas, numerical control machine tools, and flexible manipulators moving in space. Studies on related technologies of flexible servo systems have made great progress [4-6]. However, many factors are involved in flexible coupling, thus bringing great challenges to research on the control and identification of flexible servo systems.

On the basis of the above analysis, scholars have conducted extensive studies on high-precision direct-drive servo systems with flexible connections [7-8]. However, the problem of low precision of flexible coupling in the actual control of flexible linkage servo systems remains. At the same time, with the increasing size of the control system, the competition of communication resources among nodes in the system is becoming fiercer. How to reduce the waste of communication resources in the control system, overcome the limitation of communication bandwidth, and realize efficient network control has become a hot problem to be solved urgently. Therefore, how to identify and control the model parameters of flexible linkage servo systems accurately, reduce the communication resources of the networked control system, and realize the resonance

*E-mail address: tcs111@163.com

doi:10.25103/jestr.172.15

suppression of flexible linkage servo systems has important engineering implications.

Therefore, the system parameters are identified using a multi-innovation stochastic gradient (MISG) algorithm, and an event-triggered proportional-integral control for flexible linkage servo system is designed by using genetic algorithm. The genetic algorithm (GA) is introduced to optimize the control parameters, and the event-triggered (ET) mechanism with fixed threshold is employed to control the update times of the controller. Consequently, problems, such as the resonance caused by flexible coupling and the frequent update of the controller, are solved, and reference for the application, development, and optimization of flexible linkage servo systems is provided.

2. State of the art

Flexible linkage servo systems [9] consider the flexible connection between the motor and the load, making the system model accurate (compared with the rigid treatment). However, the resonance problem of flexible coupling brings challenges to the modeling and control of the system. With the recent improvement of product performance requirements, the requirements of servo drive systems are also increasing. System parameters with improved accuracy are obtained by employing various identification methods to identify system parameters, such as stochastic gradient (SG) algorithm [10], stochastic gradient identification algorithm with forgetting factor (FSG), least squares (LS) algorithm [11], and GA [12–13]. Perera et al. [14] combined SG with self-adaptation to estimate the gain matrix of adaptive parameters of motor, but the identification process only used the information of the current moment. Wei et al. [15] studied the feedback nonlinear controlled autoregressive system with SG and FSG but did not use the information before and after the identification time. Chen et al. [16] studied and analyzed the parameter identification of single inertia systems by using the LS method and Hopfield neural network algorithm through simulation experiments, but the calculation load was large and the identification process was complicated. Shi et al. [17] proposed a new gradient algorithm using multiple gradients, which accelerated the convergence speed of the method by using SW (strong wolfe) condition, but the identification accuracy must be improved further. Yuan et al. [18] proposed an H ∞ filtering algorithm with dynamic forgetting factor to identify the motor resistance and inductance online and introduced the dynamic forgetting factor into the weighted combination of the initial and current measurement noise covariance matrices, thus eliminating the identification problems caused by different initial values. However, the identification accuracy and convergence speed must be improved further.

Many servo system controls, such as proportion integration differentiation (PID) control [19], adaptive control [20], predictive control [21], and sliding mode variable structure control [22], are related to rigid connections. Omar Othman et al. [23] proposed a PID-based adaptive controller for optimizing model reference fractional order, which improved the reliability of AVR (automatic voltage regulator), but did not consider the uncertainty of the nonlinear model and system model parameters. Reza et al. [24] studied the handling and stability of all-wheel drive vehicles with priority model predictive control but did not conduct an in-depth study of the braking stability controller. To meet the high control and motion accuracy requirements of the servo system, Lian et al. [25] adopted an improved adaptive inverse method to analyze the control of the multistage electromechanical servo system, which had good robustness.

A few studies on the servo system of flexible joints mainly focus on PID control, pole placement [26], state feedback control [27], and active disturbance rejection control [28]. The core of PID control is that the tuning of controller parameters needs several tedious optimization simulation experiments, and the parameter selection is more complicated. Su et al. [29] combined the multicapacity process with PID to overcome the limitation of order and type of PID control system and realize the temperature control of the system, but the proposed method could not achieve good control effect for systems with complex coupling. Shang et al. [30] adopted the control method of combining pole placement strategy with RBF neural network, which reduced the fluctuation of the rotation angle of the flexible manipulator. However, the resonance problem between the flexible manipulator and the end effector was not well solved. To overcome the rigid body modal dynamics and realize the control of a single flexible linkage robot, Peza-Solis et al. [31] adopted the sliding mode control method to ensure the tracking of flexible state trajectories at the joint level.

In recent years, GA, particle swarm optimization, and neural networks have been employed to optimize PID control parameters. Dasari et al. [32] designed a GA-adaptive neuro fuzzy inference system-tuned PID controller, which effectively reduced the effect of sudden speed change and inertia phase change of brushless direct current motor. Hua et al. [33] used the response surface method and particle swarm optimization algorithm to improve the torque and suspension performance of the built-in bearing less permanent magnet synchronous motor. Li et al. [34] designed a direct torque control strategy of active disturbance rejection controller for a permanent magnet synchronous motor, which improved the problems of torque, flux ripple, and speed overshoot. To achieve precise positioning of magnetic coupled rodless cylinders, Zhang et al. [35] conducted an experimental study on the PID control method of RBF neural networks for magnetic coupled rodless cylinders. These control methods all adopt the traditional time-triggered control strategy, thus causing problems, such as frequent updating of controllers, waste of resources, and increase in the burden on controllers. Thus, more flexible and intelligent control strategies must be introduced.

With the rapid development of networked communication technology, an increasing number of control systems have evolved into networked control systems based on shared communication networks. The communication among sensors, controllers, and actuators in networked control systems is realized through digital communication networks. With the increasing size of the control system, the competition of communication resources among nodes in the system is becoming fiercer. How to reduce the waste of communication resources in the control system and overcome the limitation of communication bandwidth has become an urgent problem for network control technology. Aiming at the problems of network-induced delay and packet loss in networked control systems, Ndefo et al. [36–37] proposed gain scheduling PID control method and predictive control to solve the performance degradation related to NCS, but the problem of communication congestion remains.

The introduction of the ET strategy can overcome the shortcomings of periodic sampling mode and effectively solve the problem of network congestion [38]. ET control dynamically adjusts the update frequency of the controller based on the state or output of the system to realize the optimal utilization of system resources. Masroor et al. [39–40] combined the leader–follower consensus algorithm of multiagent systems with a centralized ET mechanism to realize the speed synchronization of network-coupled multimotors. Shanmugam et al. [41] proposed the stability problem of permanent magnet synchronous motor ET based on a neural network control system, which was not a sampling data controller (whether it was needed or not, sampling started at a fixed rate), avoiding unnecessary details in the transmission process to reduce computational complexity. Prakash et al. [42] proposed the ET fuzzy integral sliding mode control-based observer for nonlinear chaotic permanent magnet synchronous generators, which considered the network-induced communication constraints, and then weakened the corresponding stability problem in the sense of H∞ control performance. Song et al. [43] proposed a periodic ET control method based on GA optimization extended state observer, which solved the speed regulation problem of networked permanent magnet synchronous motor (PMSM) systems with limited communication bandwidth. At present, no study results on ET control of flexible linkage servo systems have been found.

The above studies mainly focused on the identification methods and control methods of model parameters in different fields of servo systems. On the one hand, the above algorithm only used the input and output information at the current moment to identify the system model parameters, and the identification accuracy and convergence speed must be further improved. On the other hand, studies on the control of flexible servo system, especially the systematic related study on the combination of parameter identification, control, and ET, were few. In this study, the ET mechanism is introduced into the proportional-integral (PI) control optimized by GA, and the genetic algorithm proportional-integral (GA-PI) speed control of flexible linkage servo systems based on ET is proposed. On the basis of the characteristics of flexible linkage servo systems, the multi-innovation identification of model parameters is realized by using the historical input and output speed information of the system [44–45]. The GA is employed to optimize the proportional–integral gain of PI control. To prevent excessive control energy and overshoot, the square term of control input and penalty function are introduced into the objective function of PI control optimized by GA to ensure that the system speed has less overshoot. With the increment of GA-PI speed controller taken as a variable, a decision on whether to update the output of the controller and the communication with the actuator is made by judging whether the increment error reaches the trigger threshold to save communication resources and realize the high-performance control of the system. The simulation and comparative analysis are conducted on the above traditional control methods, providing a basis for the optimization of flexible linkage servo systems.

The remainder of this study is organized as follows: Section 3 describes the characteristics and mathematical model of the flexible linkage servo system, identifies the system model parameters, and introduces the GA and ET mechanism in the speed PI control strategy. Section 4 analyzes the superiority and effectiveness of system model parameter identification and a genetic algorithm optimized proportional-integral controller with an event-triggered (ET-GA-PI) control through simulation experiments. Section 5 summarizes the conclusions. The MISG identification algorithm improves the accuracy of parameter identification of flexible linkage and is beneficial to the precise control of subsequent systems. The flexible linkage servo system controlled by ET effectively reduces the update times of the controller, reduces the operating burden of the controller, saves resources, effectively improves the disadvantages of the traditional time-triggered control method, and meets the needs of high-precision networked control.

3. Methodology

3.1 Mathematical model and resonance analysis of a flexible linkage servo system

A typical flexible linkage servo system model [9] is shown in Fig. 1. In the X_1OY_1 coordinate system, $u(x,t)$ is the deflection of the flexible load at x. In the X_0OY_0 coordinate system, $\theta_m(t)$ is the rotation angle of the servo system. T_m is the output torque of the servo system motor.

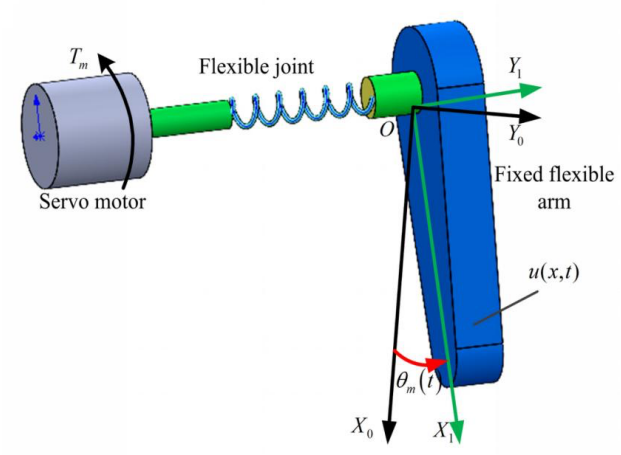

Fig. 1. Model of a flexible linkage servo drive system

When the system undergoes large-scale motion, the lateral bending vibration of the flexible beam is evident, and the longitudinal vibration is relatively negligible. When only considering the first mode, the dynamic model of the flexible linkage servo system can be expressed as

$$\begin{cases} I_a\ddot{\theta}_m + F_a\ddot{\eta} = T_m \\ \ddot{\eta} + 2\xi\Omega\dot{\eta} + \Omega^2\eta + F_a\ddot{\theta}_m = 0 \end{cases}, \quad (1)$$

where ξ is the vibration modal damping coefficient, $T_m = p_n\psi_r i_q$ is the output torque of the servo system motor, I_a is the moment of inertia of the flexible linkage, F_a is the modal coupling coefficient, Ω is the resonant frequency matrix, η is the first-order modal coordinate, $\dot{\theta}_m = \omega_m = d\theta_m/dt$ is the angular velocity of the shaft, and the corresponding acceleration is $\ddot{\theta}_m = a_m = d^2\theta_m/dt^2$. The main parameters of the system are shown in Table 1 [46].

Table 1. Main parameters of a flexible linkage servo system

Parameter	Numerical value
Motor pole logarithm p	4
Damping coefficient ξ	0.005
Permanent magnet flux Ψr/Wb	0.25
q-axis inductance Lq/mH	1.92
Armature resistance Rs/Ω	0.605
Modal frequency Ω/Hz	66
Moment of inertia of flexible load I_a/($kg \cdot m^2$)	0.0139
Coupling coefficient Fa of rotation and flexibility of high-precision instrument	0.1111

In Eq. (1), the transfer function of the system can be obtained as follows:

$$G_m(S)=\frac{\omega_m}{T_m}=\frac{1}{S}\frac{S^2+2\xi\Omega S+\Omega^2}{(I_a-F_a^2)S^2+2I_a\xi\Omega S+I_a\Omega^2}. \tag{2}$$

The flexible linkage system [46] is directly driven by the hidden pole permanent magnet synchronous motor, and the open-loop transfer function of the speed loop of the flexible linkage servo system is obtained as follows:

$$H(s)=\frac{\omega(s)}{i_q(s)}=\frac{(s^2+2\xi\Omega s+\Omega^2)p_n\psi_r}{(I_a-F_a^2)s^3+2I_a\xi\Omega s^2+I_a\Omega^2 s}. \tag{3}$$

The system speed loop control model is shown in Fig. 2.

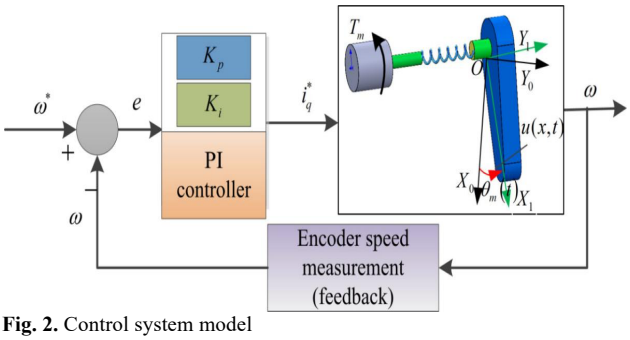

Fig. 2. Control system model

In the flexible linkage servo system, flexibility has a great influence on the speed loop. Fig. 3 shows the open-loop Bode diagram of the speed loop under flexible load. Fig. 3 shows that the resonant frequency of the flexible load is close to the bandwidth of the speed loop. Thus, the speed loop is greatly influenced by the flexible load. Similarly, the influence of flexible load on speed loop is reflected in the function of flexibility, which causes the frequency characteristic curve of the speed loop to decay at the oscillation frequency of flexible load.

3.2 Model parameter identification

The model parameters (I_a, F_a, ξ, and Ω) of the flexible linkage servo system are identified. The system discretization model is as follows:

$$\begin{aligned}\omega(k)=&-den(2)\omega(k-1)-den(3)\omega(k-2)\\&-den(4)\omega(k-3)+num(2)i_q^*(k-1)\\&+num(3)i_q^*(k-2)+num(4)i_q^*(k-3)\end{aligned}. \tag{4}$$

The parameter vectors are defined as follows:

$$\begin{aligned}\tau(k)&=[a_1(k)\ a_2(k)\ a_3(k)\ b_1(k)\ b_2(k)\ b_3(k)]^T\\&=[den(2)\ den(3)\ den(4)\ num(2)\ num(3)\ num(4)]^T\end{aligned}. \tag{5}$$

The innovation vectors are defined as follows:

$$\begin{aligned}\varphi^{\mathrm{T}}(k)=[&-\omega(k-1)\ -\omega(k-2)\ -\omega(k-3)\\&i_q^*(k-1)\ i_q^*(k-2)\ i_q^*(k-3)]^{\mathrm{T}}\end{aligned}. \tag{6}$$

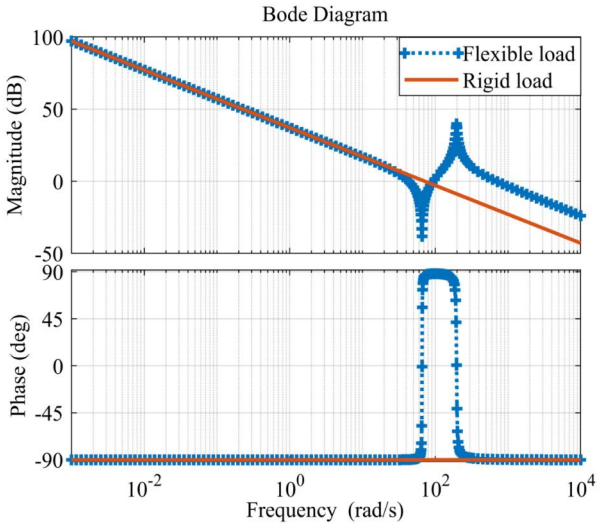

Fig. 3. Open-loop Bode diagram of the speed loop

Then, the system model can be transformed into

$$\omega(k)=\varphi^T(k)\tau(k). \tag{7}$$

Noise (assuming zero mean random noise) inevitably affects the system output measurement. Thus, the system identification model considering noise can be expressed as

$$\omega(k)=\varphi^T(k)\tau(k)+\nu(k). \tag{8}$$

The MISG identification method introduces innovation length p, which maximizes the current system speed to identify innovation and past innovation, and improves the convergence speed and identification accuracy of parameters. The identification process is shown in Fig. 4, and the parameter updating process is as follows:

$$\begin{cases}\hat{\tau}(k)=\hat{\tau}(k-1)+\dfrac{\Psi(p,k)}{r(k)}E(p,k),\hat{\tau}(0)=\dfrac{1_n}{p_0}\\ r(k)=r(k-1)+\left\|\Psi(p,k)\right\|^2,r(0)=1\\ Y(p,k)=[\omega(k),\omega(k-1),\cdots,\omega(k-p+1)]^{\mathrm{T}}\\ \Psi(p,k)=[\varphi(k),\varphi(k-1),\cdots,\varphi(k-p+1)]^{\mathrm{T}}\\ E(p,k)=Y(p,k)-\Psi^{\mathrm{T}}(p,k)\hat{\tau}(k-1)\end{cases}, \tag{9}$$

where $1_n=[1,1,\cdots,1]^T\in R^n$ is the selected large positive number, and $\kappa(k)=:1/r(k)$ is the convergence factor. The multi-innovation gradient criterion function takes

$$J(\theta):=\left\|Y(p,t)-\psi^T(p,t)\theta\right\|^2. \tag{10}$$

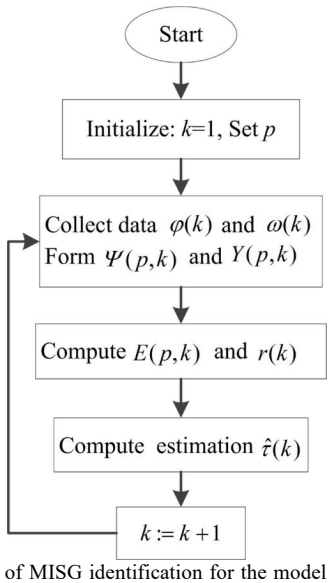

Fig. 4. Flowchart of MISG identification for the model parameters of a flexible linkage servo system.

3.3 PI control of ET speed loop for a flexible linkage servo system

3.3.1 GA-PI control

GA is used to simulate the phenomena of reproduction, crossover, and gene mutation in the process of natural selection and natural inheritance. In each iteration, a group of candidate solutions are reserved, and better individuals are selected from the candidate solution groups according to the study optimization index. Then, these individuals are combined by genetic operators (selection, crossover and mutation) to generate a new generation of candidate solution groups, and this process is repeated until the study convergence index is met. GA-PI control method optimizes PI parameters through multiple iterations and gradually approaches the optimal solution. The K_p and K_i parameters of the PI controller are taken as the optimization variables of GA, and the optimal parameter combination is found through iterative optimization to achieve the optimal performance index of the system.

The expression of discrete PI controller is as follows:

$$i_q^*(k) = K_p \cdot e(k) + K_i \sum_{j=0}^{k} e(j)T, \tag{11}$$

where K_p and K_i are parameters of the PI controller, T is the sampling period, and k is the sampling sequence number, $k = 1,2,\cdots$.

The speed tracking error is defined as follows:

$$e(k) = \omega^*(k) - \omega(k). \tag{12}$$

The discretization model of the system speed loop is as follows:

$$\begin{aligned}\omega(k) = &-den(2)\omega(k-1) - den(3)\omega(k-2)\\ &- den(4)\omega(k-3) + num(2)i_q(k-1)\\ &+ num(3)i_q(k-2) + num(4)i_q(k-3)\end{aligned}, \tag{13}$$

where $e(k)$ indicates the system speed error, $\omega^*(k)$ and $\omega(k)$ indicates the expected speed and actual output speed in the process of system control.

GA is employed to optimize the parameters K_p, K_i of the PI controller. The absolute value time integration performance index is introduced as the minimum objective function of parameter selection to obtain satisfactory speed dynamic characteristics. The square term of control input is added to the objective function to prevent the control energy from being too large. The optimal index is expressed as

$$J = \sum_{k=0}^{G} (\rho_1 |e(k)| + \rho_2 i_q^{*2}(k))kT + \rho_3 \cdot t_u. \tag{14}$$

The penalty function is adopted to avoid overshoot. If overshoot occurs, the overshoot is regarded as one of the optimal indicators. At this time, the optimal indicators are as follows:

$$J = \begin{cases} \sum_{k=0}^{G} (\rho_1 |e(k)| + \rho_2 i_q^{*2}(k))kT + \rho_3 \cdot t_u & , e\omega(k) > 0 \\ \sum_{k=0}^{G} (\rho_1 |e(k)| + \rho_2 i_q^{*2}(k) + \rho_4 |e\omega(k)|)kT + \rho_3 \cdot t_u & , e\omega(k) < 0 \end{cases} \tag{15}$$

where $i_q^*(k)$ is the output of the controller, t_u is the rising time, ρ_1, ρ_2, ρ_3, and ρ_4 are the weights, $\rho_4 >> \rho_1$, and $e\omega(k) = \omega(k) - \omega(k-1)$, $e\omega(k)$ is the change of the output speed of the system, and G is the maximum number of iterations.

3.3.2 ET mechanism

According to the error between the current moment and the next moment of the controller as the ET condition, the controller updates the data information only when the trigger condition is met, which can effectively reduce the waste of computing resources, reduce the update frequency of the controller, and lighten the burden of the actuator. When the system state does not meet the ET condition, the controller keeps the signal value generated at the latest ET. The ET strategy is designed as follows:

$$\begin{aligned} &i_q^* = i_e(t_k), \ \forall t \in [t_k, t_{k+1})\\ &t_{k+1} = \inf\{t \in R, \left|e_{i_q^*}(t)\right| \geq M\}, \ t_1 = 0 \end{aligned}, \tag{16}$$

where $0 < M < \overline{M}$, $e_{i_q^*}(t) = i_e(t) - i_q^*(t)$, $\overline{M}$ is a positive constant, M is a positive ET threshold, and $e_{i_q^*}(t)$ is the controller error.

By combining GA-PI control with ET mechanism, the speed of a flexible linkage servo system is controlled, and its control structure is shown in Fig. 5. In this system, the parameters K_p and K_i of the PI controller are iteratively optimized by GA, and the optimal parameter combination is found. In accordance with the ET mechanism, the control signal is transmitted to the flexible linkage servo system to achieve the optimal performance index of the system

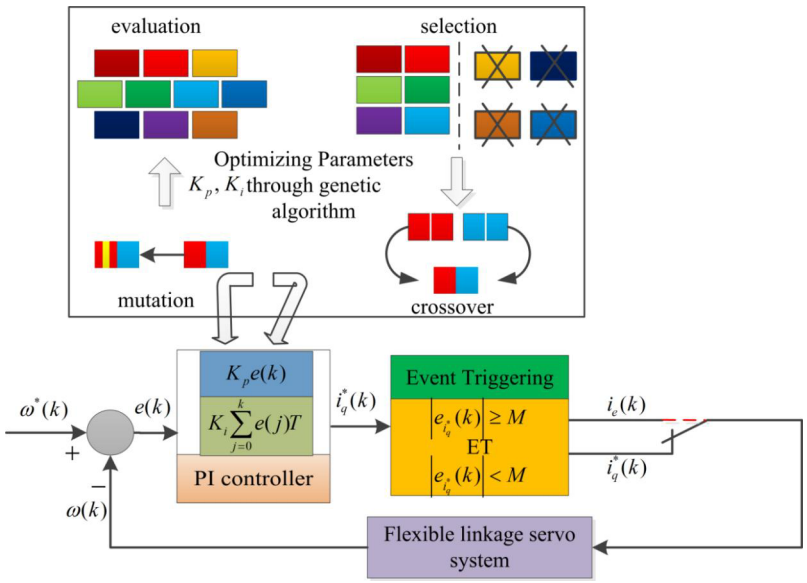

Fig. 5. ET GA-PI control strategy diagram

4. Result analysis and discussion

The effectiveness of the proposed method is verified by analyzing the parameter identification and control effect.

With model parameters brought into the system (Eq. [4]), they can be expressed as follows:

$$\begin{aligned}\omega(k) &= 2.9567\omega(k-1) - 2.9509\omega(k-2) \\ &+ 0.99427(k-3) + 0.61994\, i_q(k-1) . \\ &-1.2368\, i_q(k-2) + 0.61953\, i_q(k-3)\end{aligned} \tag{17}$$

4.1 System model parameter identification

The linear regression vector model of the system model (Eq. [17]) can be expressed as

$$\begin{aligned}&\omega(k) = \varphi^T(k)\tau(k) \\ &\tau(k) = [a_1(k)\ \ a_2(k)\ \ a_3(k)\ \ b_1(k)\ \ b_2(k)\ \ b_3(k)]^{\mathrm{T}} \\ &\varphi^T(k) = \left[-\omega(k-1) - \omega(k-2) - \omega(k-3)\, i_q(k-1)\, i_q(k-2)\, i_q(k-3)\right]^T\end{aligned} \tag{18}$$

where $\varphi^T(k)$ is the innovation vector, $\tau(k)$ is the parameter vector, and the nominal value of the corresponding parameter vector is $\tau_d = [-2.9567\ \ 2.9509\ \ -0.99427\ \ 0.61994\ \ -1.2368\ \ 0.61953]^{\mathrm{T}}$.

Traditional SG and MISG algorithms are employed to identify the parameters of the flexible linkage in the system. Tables 2 and 3 show the model parameter values, true values, and quantization errors of SG and MISG identification, respectively.

According to the simulation data in Tables 2 and 3, the following conclusions can be drawn: (1) MISG identification has high identification accuracy (measured by parameter quantization error $\delta = \left\|\hat{\tau}(k) - \tau(k)\right\| / \left\|\tau(k)\right\|$). When $k = 5000$, the parameter quantization error of the SG algorithm is $\delta_1 = 32.51282\%$, but the quantization error of the MISG algorithm decreased considerably with the increase in multi-innovation length p. When $p = 2$, $p = 3$, and $p = 4$, the identification accuracy (measured by quantization error) increased by 2.9 times ($\delta_2 = 11.14053\,\%$), 9.7 times ($\delta_3 = 3.36405\,\%$), and 26.6 times ($\delta_4 = 1.22356\,\%$), respectively, in comparison with those of the SG. (2) MISG identification has faster convergence speed than SG. When $k = 3000$, the SG algorithm ($b_1 = 0.11012$) is adopted under the same parameter b_1 (its nominal value is 0.61994), while the MISG algorithm is adopted, when $p = 2$, $p = 3$, and $p = 4$, the values of b_1 are 0.39227, 0.57723, and 0.64229, respectively. The introduction of multiple innovation length p can accelerate the convergence speed of system parameters, and the convergence speed increases with the increase in innovation length (21.6 times higher than that of the traditional SG algorithm).

Figs. 6, 7, and 8 are the model parameter estimation error curves and quantization error curves of the two methods. In Figs. 6 and 7, M2, M3, and M4 respectively represent the MISG identification of the system model parameters when $p = 2$, $p = 3$, and $p = 4$.

Table 2. SG parameter estimation and error of flexible linkage

k	a_1	a_2	a_3	b_1	b_2	b_3	δ/%
100	−0.819	1.782	−0.575	−0.269	−0.423	0.647	60.401
200	−1.039	1.900	−0.620	−0.160	−0.482	0.685	54.251
500	−1.319	2.018	−0.643	−0.064	−0.578	0.693	47.024
1000	−1.485	2.111	−0.683	0.015	−0.651	0.677	42.122
3000	−1.726	2.244	−0.728	0.110	−0.741	0.659	35.356
5000	−1.823	2.306	−0.753	0.150	−0.778	0.653	32.513
True value	−2.957	2.951	−0.994	0.620	−1.237	0.620	0

Table 3. Estimation and error of MISG parameters of flexible linkage

p	k	a_1	a_2	a_3	b_1	b_2	b_3	δ/%
2	100	−1.32868	2.62823	−1.09911	−0.08601	−1.10880	0.78922	39.94756
	200	−1.65940	2.69257	−1.10465	0.05885	−1.10120	0.81139	32.06412
	500	−2.02086	2.72437	−1.03965	0.19541	−1.12953	0.78218	23.52252
	1000	−2.20230	2.77245	−1.03332	0.28903	−1.15235	0.74380	18.82128
	3000	−2.43109	2.82194	−1.01480	0.39227	−1.17209	0.69810	13.09365
	5000	−2.50906	2.84355	−1.01382	0.42564	−1.18003	0.68349	11.14053
3	100	−2.01225	2.89814	−1.23943	0.33114	−1.05077	0.66728	22.77045
	200	−2.26325	2.92150	−1.19052	0.41640	−1.08506	0.69468	16.87294
	500	−2.53789	2.91000	−1.08088	0.48711	−1.12881	0.68648	10.26179
	1000	−2.65261	2.92715	−1.05524	0.53356	−1.16532	0.66033	7.31589
	3000	−2.77902	2.93348	−1.02515	0.57723	−1.19298	0.63947	4.22238
	5000	−2.81576	2.93682	−1.01976	0.58455	−1.20081	0.63387	3.36405
4	100	−2.46528	2.98216	−1.35579	0.70106	−0.97073	0.71814	14.89831
	200	−2.59649	2.98428	−1.22518	0.67066	−1.07162	0.70445	10.32959
	500	−2.77571	2.95999	−1.08292	0.64492	−1.13044	0.68297	5.22726
	1000	−2.83701	2.96539	−1.04755	0.64535	−1.17701	0.65106	3.30059
	3000	−2.89749	2.95501	−1.01664	0.64229	−1.20763	0.63336	1.63827
	5000	−2.91193	2.95224	−1.01185	0.63321	−1.21389	0.62894	1.22356
	True value	−2.95670	2.95090	−0.99427	0.61994	−1.23680	0.61953	0

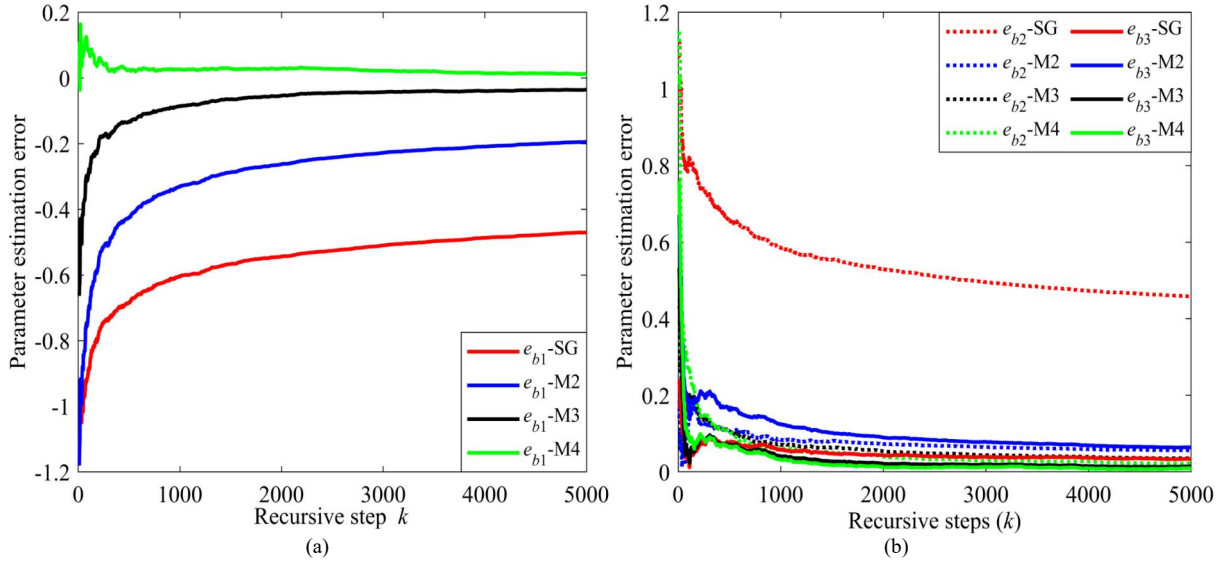

Fig. 6. Error curve of parameter (b) estimation of flexible linkage

Figs. 6, 7 and 8 show the following conclusions: (1) Compared with that of the traditional SG identification, the parameter estimation error of MISG identification ($p=3$) is smaller, and the parameter identification accuracy is higher. (2) With the increase in the length of multiple innovations, the accuracy and convergence speed of system parameter identification are remarkably improved. For the same number of iterations ($k=5000$), Fig. 8 intuitively reflects this change law, that is, the larger the length p of multiple innovations, the closer the quantization error curve is to the horizontal axis.

In addition, the forgetting factors ($FF=0.95,0.97,0.99$,respectively) were introduced into the SG algorithm to identify the model parameters of the flexible linkage servo system, and compared with the MISG algorithm ($p=4$, and $FF=1$) and the stochastic gradient algorithm ($p=1$, and $FF=1$). The quantization error curve is shown in Fig. 9.

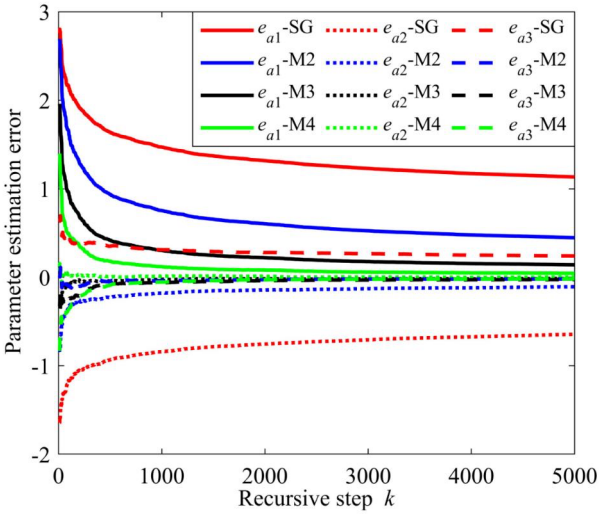

Fig. 7. Error curve of parameter (a) estimation of flexible linkage

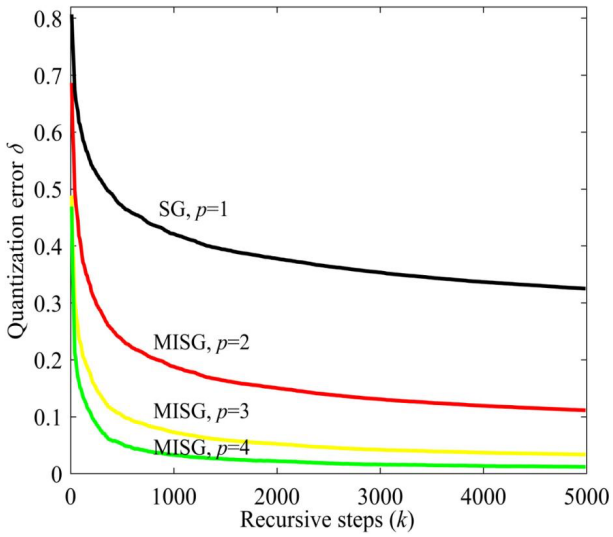

Fig. 8. Quantization error curve of the parameter estimation of flexible linkage

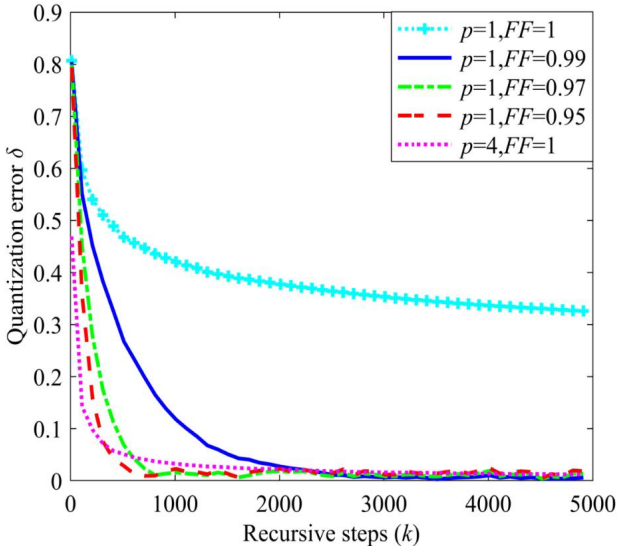

Fig. 9. Quantization error curve of parameter estimation with forgetting factor in flexible linkage

Fig. 9 shows the following conclusions: (1) With the introduction of forgetting factor (FF gradually decreases from 1 to 0.95), the quantization error of SG identification with forgetting factor quickly approaches zero, but it is slower than that of MISG. (2) With the decrease in forgetting factor, the quantization error fluctuates greatly in the steady state, which shows that the introduction of forgetting factor reduces the accuracy of model identification to a certain extent, which also reflects the contradiction between rapidity and stability in system identification. Compared with the SG with forgetting factor, MISG has higher steady-state accuracy. Therefore, it is an effective model identification method for flexible linkage servo systems.

4.2 System control performance analysis

In this study, the performance of the pole placement proportional-integral (PP-PI), second-order system engineering design proportional-integral (SSED-PI), multiple-capacity process proportional-integral (MCP-PI), and GA-PI control methods were analyzed on the basis of time trigger and ET, respectively. The sampling period of the speed loop was $T = 100\mu s$, the simulation duration was 1 s, and the input command is a step signal.

In the GA-PI control method, the number of samples was 30, and the crossover probability and mutation probability were 0.9 and 0.033, respectively. The range of K_p and K_i was [0, 1], $\rho_1 = 0.999$, $\rho_2 = 0.0001$, $\rho_3 = 0.2$, $\rho_4 = 1000$, and the iteration number G was 100.

Simulation analysis was conducted on MATLAB, and the performance of the controller was analyzed by using overshoot ($\sigma\%$), integral of squared error (ISE), integral of absolute error (IAE), and cumulative of squared control increment (CSCI). Its performance indicators are defined as follows:

$$\sigma = \frac{(M_p - M_f)}{M_f} \times 100\%, \quad ISE = \sum_{k=1}^{N} e^2(k),$$
$$IAE = \sum_{k=1}^{N} |e(k)|, \quad CSCI = \sum_{k=1}^{N} \left| i_q^{*2}(k) \right|, \tag{19}$$

where M_p is the peak value reached by the system, M_f is the steady-state value of the system, the error between the rotational speed and the set value, and the control increment. $e(k)$ is the error between the speed and the set value, and $i_q^*(k)$ is the control increment.

4.2.1 Time-triggered control

The time-triggered control mechanism is used to transmit the data signal and update the controller at a fixed time interval T. Usually, the sampling and transmission period is short, and the control signal is sent on time to realize the control of the controlled object. In this study, the sampling frequency is 10 kHz ($T = 100\mu s$), and the performance of PP-PI, SSED-PI, MCP-PI, and GA-PI control methods was analyzed on the basis of the time-triggered control mechanism within 1 s. The dynamic response is shown in Fig. 10, and the corresponding performance indicators are shown in Table 4.

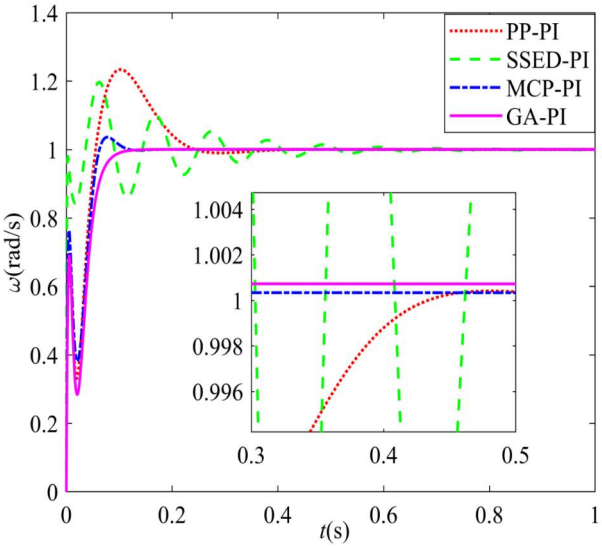

Fig. 10. Speed characteristic curve of a flexible linkage servo system

Table 4. Performance comparison of different time-triggered controllers

Method	σ%	ISE	IAE	CSCI
PP-PI	23.5368	151.4653	455.1827	6.8342e-9
SSED-PI	19.719	29.7781	278.9141	1.3426e-10
MCP-PI	3.7562	103.8896	233.2912	1.1361e-26
GA-PI	0.0726	140.7083	286.8491	4.1764e-25

Fig. 10 and Table 4 show the following conclusions: (1) With PP-PI and SSED-PI control methods, the overshoot is remarkable, reaching approximately 20%. With the MCP-PI control method, the overshoot is small. With the GA-PI control method, almost no overshoot (less than 1%) is observed, which can meet more demanding work requirements and has the optimal performance. (2) The SSED-PI method is employed to adjust the parameters. Although the speed response of the system is fast, it cannot effectively weaken the resonance generated by the system, but it produces a large overshoot and remarkable oscillation, and the system adjustment time is long. (3) The σ% of the MCP-PI and GA-PI control methods, IAE and CSCI performance indicators are superior, while the σ% of PP-PI and SSED-PI control methods, IAE and CSCI performance indicators are obviously the worst. The overshoot of the GA-PI controller is only 0.0726%, which can meet the requirement of 2% overshoot in engineering and exhibits an improved performance in the control of the speed loop of flexible linkage servo systems.

4.2.2 ET control

The ET control mechanism judges whether the difference between the current signal output by the controller at the current moment and the current signal at the next moment meets the preset ET condition according to the real-time state feedback of the system speed and then determines the update opportunity of the controller parameters. Under the ET condition of fixed threshold $M = 0.001$ and with the same sampling period $T = 100\mu s$, the performance of the above PP-PI, SSED-PI, MCP-PI, and GA-PI control methods were analyzed. The response curve of the system speed characteristic is shown in Fig. 11, and the update time of the controller output i_q is shown in Fig. 12. Table 5 shows the performance parameters of the corresponding control mode of the system.

Figs. 11 and 12 and Table 5 show the following conclusions: (1) The GA-PI controller has the optimal control performance, no remarkable overshoot, has a smooth response curve, and exhibits minimal change in dynamic performance. The SSED-PI and PP-PI methods have large overshoot, which cannot guarantee their speed and stability in the control process. By contrast, the SSED-PI method produces certain resonance but cannot suppress the system resonance. (2) Under the control of the ET mechanism, the update frequency of the controller is considerably reduced. As the system speed gradually stabilizes, the number of data updates of the controller is reduced. In accordance with the local enlarged diagram, the GA-PI controller was only updated three times between 0.86 and 0.92 s, which is far less than other control methods. The update of controller data is determined by the given trigger threshold, which reduces the waste of resources and the operating burden of the controller. (3) Among them, the performance index σ%, CSCI, and update times of the GA-PI control method are better than those of the SSED-PI, PP-PI, and MCP-PI control methods. Moreover, the overshoot of the GA-PI controller is only 0.1731% (less than 1%), which can meet the requirement of 2% overshoot in engineering. Based on the above analysis, ET-GA-PI controller has high control accuracy and stability in the speed loop control of flexible linkage servo systems.

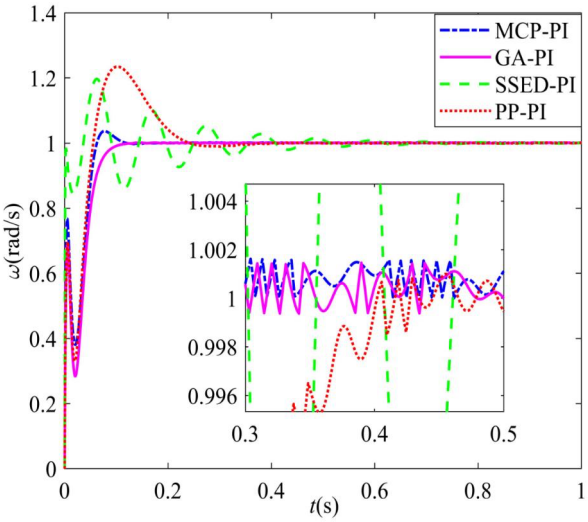

Fig. 11. Speed characteristic curve of a flexible linkage servo system

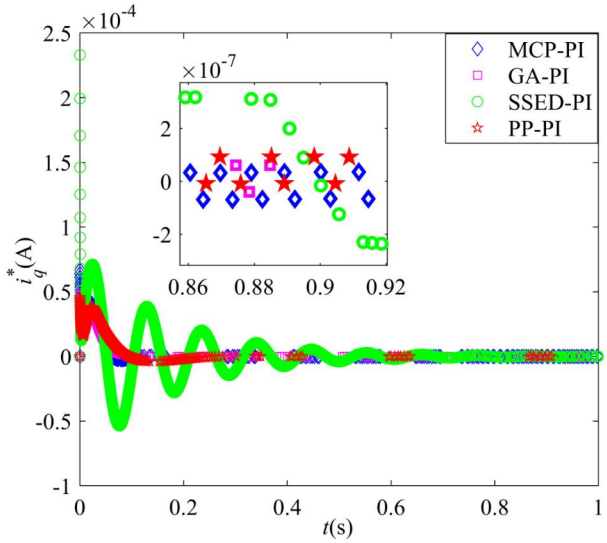

Fig. 12. Update time of controller output i_q

Table 5. Performance comparison of different controllers triggered by events

Method	σ%	ISE	IAE	CSCI	Number of updates
PP-PI	23.5045	150.7932	456.4726	0.2175	563
SSED-PI	19.7026	29.0361	277.6670	5.8547	2919
MCP-PI	3.7476	103.3607	236.0309	0.4606	637
GA-PI	0.1731	140.1288	285.3539	0.2511	524

The update frequency and data sample number of the above time-triggered control and ET control are consistent. Thus, the update time of the PI controller in this study is 10,000 times. As shown in Table 5, regardless of whether

the traditional control methods (i.e., PP-PI, SSED-PI, and MCP-PI controllers [the update times are 563, 2919, and 637, respectively]) or the GA-PI controller (the update time is 524) is used, under the ET mechanism, the number of updates of the controller is far less than that of the traditional time-triggered control.

Fig. 13 shows the change curve of update times of different controllers. Fig. 14 is a graph showing the change of the update times of the ET-GA-PI controller and the controller under the traditional continuous control method.

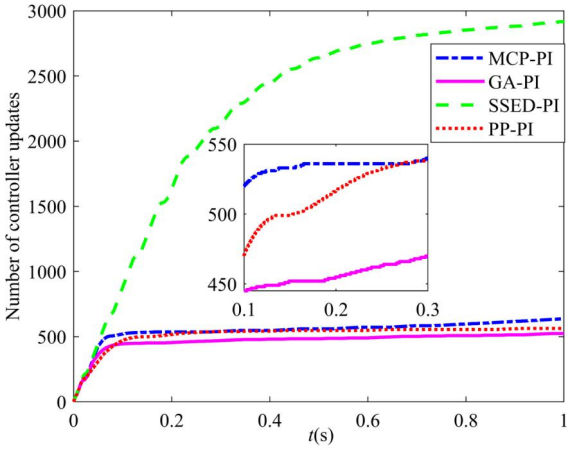

Fig. 13. Number of different controller updates

Figs. 13 and 14 show the following conclusions: (1) Under the ET mechanism, the GA-PI control method has fewer controller updates than the other three control methods and is the most superior. (2) The GA-PI controller has the least number of updates under the ET mechanism and only needs to update 524 times, which is approximately 1/20 of the traditional continuous control.

Therefore, compared with the traditional continuous control method, the ET-GA-PI controller can remarkably reduce the number of updates of the controller while ensuring the control effect, thus effectively reducing the resource consumption of the controller, further reducing the network resource consumption and lightening the burden of the controller.

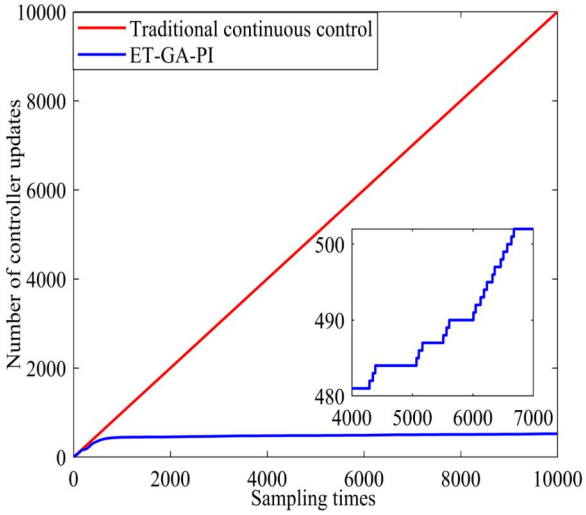

Fig. 14. Number of ET-GA-PI controller update

In ET, threshold M is the key parameter of the ET-GA-PI controller, which is closely related to the control performance and the number of controller updates. In parameter analysis, set $M \in [0.001, 0.009]$, and take five values at intervals of 0.002. The other parameters remain unchanged, and the control performance is analyzed by σ%, ISE, IAE, and CSCI, and the update times of the controller under different ET thresholds are calculated. Table 6 shows the control performance comparison of different thresholds M for ET.

Table 6 shows the following conclusions: (1) With the increase in the trigger threshold M, the update times of the ET-GA-PI controller are considerably reduced as a whole, and the control performance worsens. Among them, the σ% performance index exhibits the most remarkable deterioration, while IAE and CSCI demonstrate minimal change. (2) Overall, the indicators of the controller are ideal when the ET threshold is small, and the overall control performance is enhanced when the trigger threshold M is 0.005.

Table 6. Performance comparison of the ET-GA-PI controller with different M values

M	σ%	ISE	IAE	CSCI	Number of updates
0.001	0.1731	140.1288	285.3539	0.2511	524
0.003	0.4003	139.9867	293.8273	0.2796	346
0.005	0.5462	139.8766	302.7933	0.3315	189
0.007	0.9617	139.8132	309.2750	0.4110	166
0.009	1.2263	139.7384	321.0082	0.5232	176

5 Conclusion

The study aimed to combine organically the parameter identification of flexible linkage servo systems with the the ET control method to improve the performance and stability of the system. The problem of difficult control and frequent controller updates was evaluated by introducing a GA-PI control strategy based on the ET mechanism to improve the speed control performance of the flexible linkage servo system and reduce chattering. By using multiple innovation stochastic gradients for the parameter identification and design of an ET-GA-PI controller, the current controller was determined to be updated by designing ET conditions with fixed thresholds. On the basis of simulation experiments, the following conclusions could be drawn:

(1) The MISG identification algorithm introduces innovation length p to use effectively the input and output information of system speed at current time and historical time, thereby improving the accuracy of flexible linkage parameter identification and becoming beneficial to the accurate control of subsequent systems.

(2) Compared with time-triggered control, the ET flexible linkage servo system effectively reduces the update times of the controller, and the update times of the four control methods (i.e., PP-PI, SSED-PI, MCP-PI, and GA-PI) are all reduced by more than 70%, which reduces the operating burden of the controller, saves resources, and effectively improves the disadvantages of the traditional time-triggered control method.

(3) With the introduction of the GA, the update times of the ET-GA-PI controller can be reduced to 1/20 of the

traditional time control, with a small overshoot (0.1731%) and high control accuracy, which meets the needs of high-precision networked control.

Thus, this study combines the simulation experiment with theory, reduces the number of ETs, and saves the network resources of the system on the basis of ensuring the dynamic performance of the system, which is suitable for the network development of high-performance servo systems and has important practical implications. Given that the offline optimization algorithm cannot avoid the interference of external factors to enhance the robustness of the system, in future research, the online optimization control will be combined with this model to make the controller of the flexible linkage servo system more stable.

Acknowledgements

This work was supported by the Key Research Project of Higher Education of Henan Province in China (Grant Nos. 22B470009, 21A413005), Key Research and Development Program of Henan Province in China (Grant No. 222102210105), and Major Study and Development Project of Sichuan Province in China (Grant No.2022YFG0060).

References

[1] Y. C. Zhou, D. G. Ma, N. Y. Zhang, and H. J. Tang, "Rigidity adaptive compensation technology of alterating current servo control system," *Pow. Electron.*, vol. 55, no. 4, pp. 34-38, Apr. 2021.

[2] B. Saeid, "Advanced polynomial trajectory design for high precision control of flexible servo positioning systems," *Precis. Eng.*, vol. 84, pp. 81-90, Aug. 2023.

[3] K. Y. Liu and M. Yang, "Vibration suppression strategy of flexible joint manipulator servo system based on improved active damping," *J. Electr. Mach. Cont.*, vol. 26, no. 7, pp. 20-28, Jul. 2022.

[4] S. Kamtikar, S. Marri, B. Walt, N. K. Uppalapati, G. Krishnan, and G. Chowdhary, "Visual servoing for pose control of soft continuum arm in a structured environment," *IEEE Robot. Automat. Lett.*, vol. 7, no. 2, pp. 5504-5511, Apr. 2022.

[5] F. R. Costa Carlos and C. P. Reis João, "End-point position estimation of a soft continuum manipulator using embedded linear magnetic encoders," *Sensors-Basel*, vol. 23, no. 3, pp. 1647-1647, Feb. 2023.

[6] R. Dindorf and P. Wos, "A case study of a hydraulic servo drive flexibly connected to a boom manipulator excited by the cyclic impact force generated by a hydraulic rock breaker," *IEEE Access*, vol. 10, pp.7734-7752, Jan. 2022.

[7] K. Takumi, *et al*, "Design of servo valve using buckled tubes for desired operation of flexible robot arm based of static analytical model," *Int. J. Fluid Pow. Syst.*, vol. 15, no. 3, pp. 86-94, Jan. 2022.

[8] M. Merlin, B. Markus, S. Robert, and E. Peter, "End-effector trajectory tracking of flexible link parallel robots using servo constraints," *Multibody Syst. Dyn.*, vol. 56, no. 1, pp. 1-28, Jul. 2022.

[9] D. Y. Shang, X. P. Li, M. Yin, and F. J. Li, "Dynamic modeling and control for dual-flexible servo system considering two-dimensional deformation based on neural network compensation," *Mech. Mach. Theory*, vol. 175, pp. 49-54, Jun. 2022.

[10] H. M. Xing, F. Ding, and F. Pan, "Auxiliary model-based hierarchical stochastic gradient methods for multiple-input multiple-output systems," *J. Comput. Appl. Math.*, vol. 442, pp. 115687-115687, Jul. 2024.

[11] Z. Anwar, B. Ahmed, B. Bachir, K. Katia, and B. Mohammed, "New identification of induction machine parameters with a meta-heuristic algorithm based on least squares method," *Compel.*, vol. 42, no. 6, pp. 1852-1866, Nov. 2023.

[12] J. Jens, F. Christian, and R. Stephan, "System identification of a gyroscopic rotor throughout rotor-model-free control using the frequency domain LMS," *IFAC PapersOnline*, vol. 55, no. 25, pp. 217-222, Jan. 2022.

[13] K. Shiu and S. Alok, "A new parameter tuning approach for enhanced motor imagery EEG signal classification," *Med. Biol. Eng. Comput.*, vol. 56, no. 10, pp. 1861-1874, Apr. 2018.

[14] A. Perera and R. Nilsen, "A framework and an open-loop method to identify PMSM parameters online," *in Proc. 23rd Int. Conf. Electr. Mach. Syst.*, Hamamatsu, H, Japan, 2020, pp. 1945-1950.

[15] C. Wei, L. Xu, and F. Ding, "Stochastic gradient identification algorithm for feedback nonlinear systems and its convergence," *Con. Theor. Appl.*, vol. 40, no. 10, pp. 1757-1764, May. 2023.

[16] Z. H. Chen and Y. Q. Wang, "Study on parameter identification of single inertia servo drive system," *Mod. Mach. Tool Automat. Manuf. Technol.*, no. 10, pp. 40-42+48, Oct. 2023.

[17] Y. Q. Shi and S. X. Jing, "Strong Wolfe condition-based variable stacking length multi-gradient parameter identification algorithm," *Int. J. Model. Identif.*, vol. 41, no. 4, pp. 289-294, Jan. 2022.

[18] T. Q. Yuan, J. Chang, and Y. P. Zhang, "Parameter identification of permanent magnet synchronous motor with dynamic forgetting factor based on H∞ filtering algorithm," *Actuators*, vol. 12, no. 12, pp. 453-453, Dec. 2023.

[19] A. H. Mintsa, E. G. Eny, N. Senouveau, and R. M. A. Nzué, "Optimal tuning PID controller gains from ziegler- nichols approach for an electrohydraulic servo system," *J. Eng. Res. Rep.*, vol. 25, no. 11, pp. 158-166, Dec. 2023.

[20] M. Jovan and S. Timothy, "Discerning discretization for unmanned underwater vehicles DC motor control," *J. Mar. Sci. Eng.*, vol. 11, no. 2, pp. 436-436, Feb. 2023.

[21] B. Aydn, K. Ersan, and K. Yasin, "Model predictive torque control-based induction motor drive with remote control and monitoring interface for electric vehicles," *Electr. Pow. Compo. Sys.*, vol. 51, no. 18, pp. 2159-2170, Oct. 2023.

[22] A. A. G. Mahmoud A., A. Almoataz Y., A. Ziad M., and D. A. A. Zaki, "A comprehensive examination of vector-controlled induction motor drive techniques," *Energies*, vol. 16, no. 6, pp. 2854-2854, Mar. 2023.

[23] A. M. Omar Othman, I. Marei Mostafa, and A. Attia Mahmoud, "Comparative study of AVR control systems considering a novel optimized PID-based model reference fractional adaptive controller," *Energies*, vol. 16, no. 2, pp. 830-830, Jan. 2023.

[24] H. Reza, K. Amir, K. Alireza, C. S. Ken, and L. Bakhtiar, "A prioritisation model predictive control for multi-actuated vehicle stability with experimental verification," *Vehicle Syst. Dyn.*, vol. 61, no. 8, pp. 2144-2163, Aug. 2023.

[25] Y. X. Lian, Y. Zhou, J. X. Zhang, S. J. Ma, and S. Wu, "An Intelligent nonlinear control method for the multistage electromechanical servo system," *Appl. Sci.*, vol. 12, no. 10, pp. 5053-5053, May. 2022.

[26] X. C. Liu, Y. H. Wang, and M. H. Wang, "Speed fluctuation suppression strategy of servo system with flexible load based on pole assignment fuzzy adaptive PID," *Mathematics-Basel*, vol. 10, no. 21, pp. 3962-3962, Oct. 2022.

[27] S. Madanzadeh, A. Abedini, A. Radan, and J. S. Ro. "Application of quadratic linearization state feedback control with hysteresis reference reformer to improve the dynamic response of interior permanent magnet synchronous motors," *ISA T.*, vol. 99, pp. 167-190, Apr. 2020.

[28] W. T. Gyeom, K. B. Jin, and Y. Y. Doo, "Mechanical resonance suppression method based on active disturbance rejection control in two-mass servo system," *J. Pow. Electron.*, vol. 22, no. 8, pp. 1324-1333, Jun. 2022.

[29] J. C. Su and P.Yang, "Cascade MCP-PID control of superheated steam temperature," *Automat. Instrum.*, vol. 35, no. 11, pp. 5-8, Nov. 2014.

[30] D. Y. Shang, X. P. Li, M. Yin, and F. J. Li, "Control Method of Flexible Manipulator Servo System Based on a Combination of RBF Neural Network and Pole Placement Strategy," *Mathematics-Basel*, vol. 9, no. 8, pp. 896-896, Apr. 2021.

[31] J. F. Peza-Solis, G. Silva-Navarro, O. A. Garcia-Perez, and L.G. Trujillo-Franco, "Trajectory tracking of a single flexible-link robot using a modal cascaded-type control," *Appl. Math. Model.*, vol. 104, pp. 531-547, Jan. 2022.

[32] M. Dasari, A. Srinivasula Reddy, and M. Vijaya Kumar, "GA-ANFIS PID compensated model reference adaptive control for BLDC motor," *Int. J. Pow. Electron. Drive Syst.*, vol. 10, no. 1, pp. 265-276, Jan. 2019.

[33] Y. Z. Hua, Y. C. Liu, W. Pan, X. Y. Diao, and H. Q. Zhu, "Multi-objective optimization design of bearingless permanent magnet synchronous motor based on improved particle swarm optimization algorithm," *J. China Electr. Eng.*, vol. 43, no. 11, pp. 4443-4452, Apr. 2023.

[34] S. P. Li, Y. Xie, K. Zhang, and Y. T. He, "Direct torque control of permanent magnet synchronous motor based on active disturbance rejection controller," *Electr. Meas. Instrum.*, vol. 61, no. 1, pp. 195-200, Jan. 2024.

[35] Y. M. Zhang, *et al*, "Nonlinear control of magnetically coupled rodless cylinder position servo system," *Chin. J. Mech. Eng-en.*, vol. 36, no. 1, pp. 145-145, Dec. 2023.

[36] M. I. Ndefo, S. C. Nwafor, C. C. Udeze, O. Akpeghagha, and O. C. Ugbe, "Performance evaluation of networks using gain scheduling PID networked control system for nonlinear systems," *J. Eng. Res. Rep.*, vol. 25, no. 5, pp. 17-30, Jul. 2023.

[37] M. Haritha, G. Sandip, and K. Shyam, "Predictive control of networked control system with event-triggering in two channels," *Eur. J. Control*, Accessed: Apr. 18, 2023. [Online.] Available:https://www.sciencedirect.com/science/article/abs/pii/S0947358023000390.

[38] Y. Bai and Y. W. Jing, "Event-triggered network congestion control of TCP/AWM systems," *Neural Comput. Appl.*, vol. 33, no. 22, pp. 15877-15886, Jul. 2021.

[39] S. Masroor, P. Chen, Z. A. Ali, and F. M. Mahomed, "Event triggered multi-agent consensus of DC motors to regulate speed by LQR scheme," *Math. Comput. Appl.*, vol. 22, no. 1, pp. 14-14, Jul. 2017.

[40] S. Masroor and P. Chen, "Event triggered non-inverting chopper fed networked DC motor speed synchronization," *Compel*, vol. 37, no. 2, pp. 911-929, Mar. 2018.

[41] L. Shanmugam, P. Mani, and H. Y. Joo, "Stabilisation of event-triggered-based neural network control system and its application to wind power generation systems," *Inst. Eng. Technol. Con. Theor. Appl.*, vol. 14, no. 10, pp. 1321-1333, Jul. 2020.

[42] M. Prakash, R. Rakkiyappan, and Y. J. Hoon, "Design of observer-based event-triggered fuzzy ISMC for T-S fuzzy model and its application to PMSG," *IEEE Trans. Syst. Man. Cybern. Syst.*, vol. 51, no. 4, pp. 1-11, Jul. 2019.

[43] J. Song, Y. K. Wang, Y. Niu, H. K. Lam, S. He, and H. Liu, "Periodic event-triggered terminal sliding mode speed control for networked PMSM system: a GA-optimized extended state observer approach," *IEEE-ASME T. Mech.*, vol. 27, no. 5, pp. 4153-4164, Apr. 2022.

[44] L. Xu, F. Ding, Y. Gu, A. Alsaedi, and T. Hayat, "A multi-innovation state and parameter estimation algorithm for a state space system with d-step state-delay," *Signal Process.*, vol. 140, pp. 97-103, Nov. 2017.

[45] Q. Y. Shen and F. Ding, "Multi-innovation parameter estimation for Hammerstein MIMO output-error systems based on the key-term separation," *IFAC PapersOnline*, vol. 48, no. 8, pp. 457-462, Feb. 2015.

[46] Y. S. Ding and X. Xiao, "Control method of flexible load directly driven by permanent magnet synchronous motor," *Trans. China Electrotech. Soc.*, vol. 32, no. 4, pp. 123-132, Feb. 2017.